IEEE Access
Multidisciplinary ⋮ Rapid Review ⋮ Open Access Journal

Received 17 February 2024, accepted 29 February 2024, date of publication 27 March 2024, date of current version 4 April 2024.

Digital Object Identifier 10.1109/ACCESS.2024.3382208

RESEARCH ARTICLE

Enhanced Unknown System Dynamics Estimator With Measurement Noise Rejection for Series Elastic Actuators

CHENGHUAN LI[1,3], SIYU CHEN[2,3], JING NA[2,3], (Member, IEEE), YINGBO HUANG[2,3], AND JUN MA[1,3]

[1]Faculty of Information Engineering and Automation, Kunming University of Science and Technology, Kunming 650500, China
[2]Faculty of Mechanical and Electrical Engineering, Kunming University of Science and Technology, Kunming 650500, China
[3]Yunnan Key Laboratory of Intelligent Control and Application, Kunming University of Science and Technology, Kunming 650500, China

Corresponding author: Jing Na (najing25@163.com)

This work was supported in part by the National Natural Science Foundation of China under Grant 62273169 and Grant 62373174; and in part by Yunnan Fundamental Research Projects under Grant 202001AV070001, Grant 202201AW070005, Grant 202202AG050012, Grant 202101BE070001-060, and Grant 202101BE070001-055.

ABSTRACT Implementing the model-based control strategies for Series Elastic Actuators (SEAs) is not an easy task due to the unknown system dynamics in their force models such as modeling uncertainties and external disturbances. In this paper, an enhanced unknown system dynamics estimator (EUSDE) is presented for the SEAs to online estimate the lumped unknown system dynamics in real time with guaranteed convergence and noise rejection response. The proposed approach is an extension of our previously developed unknown system dynamics estimator (USDE). The key idea is to further address the sensitivity of the USDE to measurement noise to further enhance the estimation performance. In this line, a high-order filter is introduced to the design and analysis of USDE. Moreover, this study also provides a comparative analysis of USDE and EUSDE from both the time-domain and frequency-domain perspectives. Finally, comparative simulation and experimental results are provided to demonstrate the effectiveness of the proposed methods.

INDEX TERMS Series elastic actuator, unknown system dynamics estimator, measurement noise rejection, frequency-domain analysis.

I. INTRODUCTION

As the human-computer interaction is more widely used in the robotic operation, conventional position control technologies are inadequate to satisfy the ever-increasing high-performance control requirements of robots. In this sense, the design of actuators with precise force feedback is emerging. In addition, considering the issue of safety, biomechanical flexibility/compliance should be suggested in the actuators, which contributes to providing effective buffering when robots encounter unexpected impacts. To accomplish these objectives, series elastic actuators (SEAs) were initially proposed by Pratt et al. [1], in which the elastic elements between the load and the actuating motor are integrated. Recently, the SEAs have been widely implemented in numerous robotic products such as rehabilitation robots, humanoid robots and mechanical exoskeletons, e.g., [2], [3], [4].

To achieve a satisfactory operation performance, various control strategies have been developed for SEAs. For instance, Vantilt et al. [5] proposed a model-based control method, which utilizes a dynamic model of SEAs to compensate for its inherent dynamics. However, considering the inherent complexity of force control, how to derive a high precision model of SEAs has been an emerging topic. In fact, it has been well recognized that the model-based approaches all presume an accurate description of SEA dynamics. Nevertheless, due to the extensive operations

The associate editor coordinating the review of this manuscript and approving it for publication was Haibin Sun.

of SEA in robotic products, there are inevitably modeling uncertainties in the existing mathematical models of practical SEA systems. Hence, the consideration of internal/external disturbances, modeling uncertainty and even measurement noise (note that in this study we uniformly call those factors as the unknown system dynamics) is essential for precise motion control of such equipments, which has attracted great attentions from both academic and industrial communities.

To address the aforementioned issue of the unknown system dynamics, an intuitive way is to estimate and then compensate the lumped system uncertainties via feedforward control schemes. In this line, the disturbance-observer-based control [6] was well recognized. In [7], an original disturbance observer (DOB) was reported for linear systems in the early 1980s by Ohishi et al., the core idea of which is to design a low-pass filter based observer in the frequency-domain to estimate the unknown dynamics. The extension of DOB to nonlinear systems was subsequently proposed (please refer to [6] for more detailed references). Apart from this idea, Han [8] also proposed the well-known extended state observer (ESO), which takes the lumped dynamics as a new system state and then reconstructs them via an observer [9]. These two approaches were also integrated into the control of SEAs. Paine et al. [10] addressed the uncertainties in a generic SEA model, and then presented a model-based control with a DOB. Yu et al. [11] also proposed an ESO-based optimal control with friction compensation and disturbance rejection to improve tracking precision for force control of SEAs. Nevertheless, to simplify the tedious parameter tuning, the authors of [12] further developed an enhanced ESO strategy, where the control parameters can be tuned with the eigenvalue assignment technique and bandwidth. Although the above methods have achieved satisfactory estimation results, the design and implementation of such estimators are still somehow tedious, where the parameter tuning was not fully solved yet. To address this problem, a simple, fast and robust estimator named unknown system dynamics estimator (USDE) was proposed in our previous work [13], [14]. In this framework, a filter operator is first introduced to reconstruct the derivative information of system state, and then the estimator is designed based on an invariant manifold, such that only a scalar needs to be set by the designers with an intuitive guideline. This USDE provides an alternative approach to handle the system uncertainties, whose convergence proprieties are comparable to DOB and ESO [13]. Thus, the USDE has recently been used in various control designs [15], [16], [17], where the estimator is adopted as a feedforward control action. However, the USDE may suffer from the sensitivity to measurement noise in practical applications with sufficiently small filter constants and it may even trigger the instability of the closed-loop system [14]. Note that similar issues were also concerned in the design of other observers. In [18], Sariyildiz and Ohnishi pointed out that the rejection of noise can be improved by increasing the order of DOB. For high-gain observers, Astolfi et al. [19] proposed a pre-filtering method to handle the effect of measurement noise. Recently, Han et al. [12] reported a modified ESO to achieve rejection of noise in a low-stiffness SEA. However, it remains as an open problem to design an alternative USDE with enhanced robustness against measurement noise.

Based on the above discussions, an enhanced unknown system dynamics estimator (EUSDE) is developed to estimate the lumped unknown system uncertainties of SEAs, where the effects of the high-frequency measurement noise can be suppressed. Specifically, a SEA model described as a second-ordered system is considered, and the sensitivity of the USDE initially given in [13] and [14] concerning on the measurement noise is analyzed. Then a higher-order filter is introduced to tailor the USDE as the EUSDE. To show the effectiveness and superiority of the suggested EUSDE, a comparative analysis from both the time-domain and frequency-domain perspectives is carried out. Finally, comparative simulations and experiments are conducted based on a SEA test-rig to demonstrate the superiority of the proposed methods.

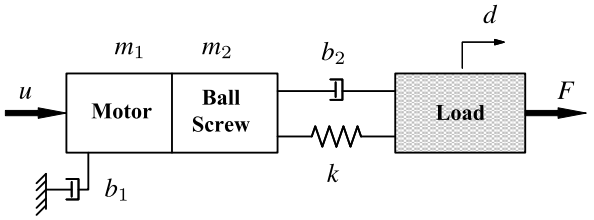

FIGURE 1. Simplified modeling of linear SEAs.

II. PROBLEM FORMULATION

In this paper, the studied SEA consists of a servomotor, a ball crew and a translational spring which is connected between the ball screw nut and the external load. The schematic of the SEA is depicted in Fig. 1 and its dynamic model can be obtained based on the Newton's second law as [11]:

$$\ddot{F} = -\frac{k}{m}F - \frac{b_1 + b_2}{m}\dot{F} + \frac{\mu k}{m}u + h, \tag{1}$$

where F is the actuator output force, $m = m_1 + m_2$ is the total equivalent mass of the motor m_1 and the ball screw m_2 in terms of translational motion, u is the motor input current, b_1 and b_2 denote the damping coefficients, μ is the motor torque coefficient between the current and the force, k is the spring elastic coefficient, and h denotes the lumped unknown system dynamics including the modeling uncertainties and external disturbances.

For the ease of the subsequent analysis, we choose the state variables as $x_1 = F, x_2 = \dot{x}_1$, such that the state-space form of system (1) can be written as:

$$\begin{cases} \dot{x}_1 = & x_2, \\ \dot{x}_2 = & \phi(x, u) + h, \end{cases} \tag{2}$$

where $\phi(x, u) = -\frac{k}{m}x_1 - \frac{b_1+b_2}{m}x_2 + \frac{\mu k}{m}u$.

The problem to be addressed is to estimate the lumped unknown system dynamics h including the modeling uncertainties and external disturbances by using the input u and measurable/observed output $x = [x_1, x_2]$.

Without loss of generality, the following assumptions on system (2) are given to guarantee that there exists a unique solution to the studied problem.

Assumption 1: The states x and the lumped unknown dynamics h of system (2) are bounded. Moreover, the derivative of h is also bounded, i.e., $\sup_{t\geq 0}|\dot{h}| \leq \hbar_1$ holds for a positive constant $\hbar_1 > 0$.

Remark 1: The above assumption on system (2) is practically feasible for SEAs as claimed in [11] and [12] and thus it has been widely used in the design of estimators [6], [8], [13]. Specifically, a proper control u can be adopted to ensure the boundedness of system states and unknown dynamics. Moreover, although the well-known DOB [6] and ESO [8] can be used to solve the studied problem, the parameter tuning of such estimators is slightly complex. Nevertheless, the recently proposed USDE [13], [14] whose convergence response is comparable to DOB and ESO can also be used herein, while its robustness against high-frequency measurement noise remains as an interesting topic to be further addressed in this paper.

III. FURTHER ANALYSIS ON USDE AND MOTIVATIONS

In this section, we will recall the design of USDE, which was initially reported in our previous work [13], [14], and particularly analyze the robustness against the measurement noise.

A. UNKNOWN SYSTEM DYNAMICS ESTIMATOR

Different to the design of ESO, which takes the unknown dynamics as an augmented system state, we first apply a first-order low-pass filter on the output x_2 and known dynamics ϕ as:

$$\kappa\dot{x}_{2f} + x_{2f} = x_2, \quad \kappa\dot{\upsilon}_f + \upsilon_f = \phi, \tag{3}$$

where $\kappa > 0$ is a manually set constant. Note that the initial values of filters, i.e., $x_{2f}(0)$, $\upsilon_f(0)$ are set to zero.

According to the constructed invariant manifold in [20], the estimator, namely USDE, is designed as follows:

$$\hat{h} = \frac{x_2 - x_{2f}}{\kappa} - \upsilon_f, \tag{4}$$

where $\hat{h}$ denotes the estimate of the unknown system dynamics h.

To show the key merit of the proposed USDE (4), the frequency-domain analysis is performed (ignoring the vanishing effects of the initial values $x_2(0)$). Hence, this estimator (4) can be reformulated with the Laplace transform $\mathcal{L}\{\cdot\}$ and (2) as:

$$\begin{aligned}\hat{H} &= \frac{s}{\kappa s+1}X_2 - \frac{1}{\kappa s+1}V \\ &= \frac{1}{\kappa s+1}H,\end{aligned} \tag{5}$$

where $\hat{H}, H, X_2, V$ are the Laplace transformed variables of $\mathcal{L}\{\hat{h}\}, \mathcal{L}\{h\}, \mathcal{L}\{x_2\}, \mathcal{L}\{\upsilon\}$, respectively.

Define the estimation errors as $\tilde{h} = h - \hat{h}$ and $\tilde{H} = \mathcal{L}\{\tilde{h}\}$, then one can derive that:

$$\tilde{H} = \frac{\kappa s}{\kappa s+1}H. \tag{6}$$

As shown in (5), the estimate $\hat{h}$ equals to $\hat{h} = h_f$ with $\kappa\dot{h}_f + h_f = h$. Hence, as shown in (6), there exists an arbitrarily small compact set $\Omega_1 = \{|\tilde{h}| \leq \delta, \delta \geq 0\}$ including the origin $\tilde{h} = 0$, such that for any $\kappa > 0$, one can claim that $\tilde{h} \in \Omega$ for $t > T$ for a finite time $T > 0$. Specifically, if $\hbar_1 \to 0$ (i.e., the unknown dynamics h is constant) and $\kappa \to 0$ is sufficiently small, the estimation error $\tilde{h}$ converges to zero, i.e., $\delta \to 0$. The convergence property of the estimator (4) is summarized as the following theorem [13], [14]:

Theorem 1: Considering system (2) with Assumption 1, the USDE (4) is used, then the estimation error $\tilde{h}$ converges to a small compact set, whose size depends on $\hbar_1, \kappa$.

Proof: By applying the inverse Laplace transform on (6), we can derive the error dynamics in the time-domain as:

$$\dot{\tilde{h}} = -\frac{1}{\kappa}\tilde{h} + \dot{h}. \tag{7}$$

Choosing a Lyapunov function as $V_1 = \frac{1}{2}\tilde{h}^2$, then its time derivative can be calculated as:

$$\dot{V}_1 = -\frac{1}{\kappa}\tilde{h}^2 + \tilde{h}\dot{h}. \tag{8}$$

Based on the Young's inequality $\tilde{h}\dot{h} \leq \tilde{h}^2/(2\kappa) + \kappa\dot{h}^2/2$, we can further derive:

$$\dot{V}_1 \leq -\frac{1}{\kappa}V_1 + \frac{\kappa}{2}\hbar_1^2. \tag{9}$$

Then recalling the Comparison Lemma [21] with respect to (9), we can obtain that

$$V_1(t) \leq e^{-\frac{t}{\kappa}}V_1(0) + \frac{\kappa^2\hbar_1^2}{2}. \tag{10}$$

Therefore, it can be concluded that

$$\Omega_1 = \left\{\tilde{h} \mid |\tilde{h}|^2 \leq 2e^{-\frac{t}{\kappa}}|\tilde{h}(0)|^2 + \kappa^2\hbar_1^2\right\}, \tag{11}$$

From the above analysis, we can claim that the estimation error $\tilde{h}$ is bounded and will converge to a small compact set, whose size depends on the filter constant κ and the variation rate of unknown dynamics $\hbar_1$ defined in Assumption 1. Specifically, it can be further deduced that the condition $\lim_{t\to\infty}\Omega_1 = 0$ can be fulfilled provided that $\kappa \to 0$ and/or $\hbar_1 \to 0$.

Remark 2: As shown in Theorem 1, one can find that the convergence properties in terms of both convergent rate and ultimate error bound are comparable to those of DOB [6] and ESO [8], which are better than the sliding mode estimator and dirty differentiation estimator given in [20]. Moreover, only a constant κ needs to be set for the developed USDE, whose parameter tuning is a more trivial task than that of DOB and ESO. Nevertheless, following the proof of Theorem 1, we have a conclusion that choosing a small κ can contribute to guaranteeing the fast convergence rate and better estimation accuracy. However, when the system measurement x_2 is perturbed by high-frequency measurement noise, its effect may be amplified and thus the estimation performance may be deteriorated, which has been preliminarily studied in [20]. To further investigate this issue, the robustness analysis of the USDE will be revisited in the next subsection.

B. ROBUSTNESS ANALYSIS OF USDE

Now the robustness of the USDE (4) against the measurement noise is studied. In this line, we assume that the system state x_2 suffers from a bounded measurement noise ϵ_1, such that the available variable used for the design of USDE is given by:

$$\bar{x}_2 = x_2 + \epsilon_1. \tag{12}$$

Besides, to better elaborate the influence of measurement noise on system (2), we denote ϵ_2 as a composite error arising from the noise perturbed in the states x_1, x_2 in $\phi(x, u)$ and the control input u, such that the other variable used for the design of USDE is given as follows:

$$\bar{\upsilon} = \phi + \epsilon_2. \tag{13}$$

In this case, the filter operation (3) can be rewritten as:

$$\kappa \dot{\bar{x}}_{2f} + \bar{x}_{2f} = \bar{x}_2, \quad \kappa \dot{\bar{\upsilon}}_f + \bar{\upsilon}_f = \bar{\upsilon}. \tag{14}$$

and the USDE can be reformulated as:

$$\hat{h} = \frac{\bar{x}_2 - \bar{x}_{2f}}{\kappa} - \bar{\upsilon}_f. \tag{15}$$

Now, we examine the influence of measurement noise on the USDE (15) using the frequency-domain analysis. Let $E_1 = \mathcal{L}\{\epsilon_1\}$ and $E_2 = \mathcal{L}\{\epsilon_2\}$, and consider the estimation error of (15) in the frequency-domain as:

$$\tilde{H} = P_1 H - P_2 E_1 + P_3 E_2, \tag{16}$$

where the transfer functions P_1, P_2, P_3 are given as:

$$P_1 = \frac{\kappa s}{\kappa s + 1}, \quad P_2 = \frac{s}{\kappa s + 1}, \quad P_3 = \frac{1}{\kappa s + 1}. \tag{17}$$

Compared with (6), it is found that in addition to the term with P_1 determining the estimation error associated with H, there are other two residual terms with P_2 and P_3 denoting the effect of ϵ_1 and ϵ_2, respectively. From (16), the measurement noise ϵ_1 and ϵ_2 affects the estimation error in a non-uniform manner. Since $P_3 = \frac{1}{\kappa s+1}$ is indeed a low-pass filter, the influence of ϵ_2 on the estimation error can be diminished with a small κ. Hence, we will examine the influence of ϵ_1 on the estimation error by plotting the frequency response of P_2 as given in Fig. 2. It can be found that amplitude of P_2 increases along with the decrease of filter constant κ, hence the effects of noise ϵ_1 in x_2 can be amplified in the estimation error $\tilde{h}$, which limits the performance of (15). Therefore, the constant κ cannot be set too small, which in turn can increase the ultimate bound of error $\tilde{h}$.

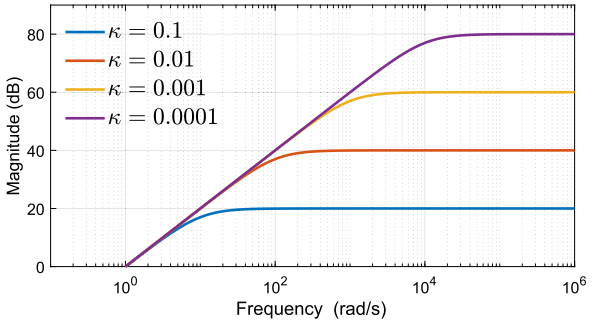

FIGURE 2. The frequency response of P_2 with EUSDE (15).

In the presence of measurement noise, the convergence property of USDE (15) can be concluded as follows.

Theorem 2: Considering system (2) with measurement noise in (12) and (13), the estimation error $\tilde{h}$ of USDE (15) converges to a compact set, whose size is determined by the amplitude of noise.

Proof: According to (16), the estimation error $\tilde{h}$ can be described in the time-domain as:

$$\dot{\tilde{h}} = -\frac{1}{\kappa}\tilde{h} + \dot{h} - \frac{1}{\kappa}\dot{\epsilon}_1 + \frac{1}{\kappa}\epsilon_2. \tag{18}$$

Choosing a Lyapunov function as $V_2 = \frac{1}{2}\tilde{h}^2$, then the derivative of V_2 with respect to time t can be derived along with (18) as:

$$\dot{V}_2 = -\frac{1}{\kappa}\tilde{h}^2 + \tilde{h}(\dot{h} - \frac{1}{\kappa}\dot{\epsilon}_1 + \frac{1}{\kappa}\epsilon_2). \tag{19}$$

By applying the Young's inequality, one can obtain:

$$\begin{aligned}\dot{V}_2 \leq & -\frac{1}{2\kappa}\tilde{h}^2 + \frac{\kappa}{2}(\dot{h} - \frac{1}{\kappa}\dot{\epsilon}_1 + \frac{1}{\kappa}\epsilon_2)^2 \\ \leq & -\frac{1}{\kappa}V_2 + \frac{\kappa}{2}(\hbar + \Xi_1)^2,\end{aligned} \tag{20}$$

with $\Xi_1 = \kappa^{-1}(|\dot{\epsilon}_1| + |\epsilon_2|)$ being the upper bounds of the noise $\dot{\epsilon}_1, \epsilon_2$, such that

$$V_2(t) \leq e^{-\frac{t}{\kappa}}V_2(0) + \frac{\kappa^2}{2}(\hbar + \Xi_1)^2. \tag{21}$$

To this end, we can conclude that the estimation error $\tilde{h}$ is bounded and will converge to a compact set defined by

$$\Omega_2 = \left\{\tilde{h} \mid |\tilde{h}|^2 \leq 2e^{-\frac{t}{\kappa}}|\tilde{h}(0)|^2 + \kappa^2(\hbar + \Xi_1)^2\right\}. \tag{22}$$

Clearly, as shown in (22), the ultimate bound of estimation error depends on the variation rate of ϵ_1 and amplitude of ϵ_2, apart from the variation rate of unknown dynamics. More

specifically, as given in the definition of Ξ_1, one can find that the filter constant κ cannot be set too small in order to retain certain value of Ξ_1 to ensure fair estimation performance. This also supports the claim in Remark 1 and the observations given in Fig.2 derived from the frequency-domain analysis.

To support the above analysis, a typical example is further studied. It is noted that the noise to be attenuated in the operation of SEAs mainly stem from the hardware measurement of system states, where the main components are located in the high-frequency band. Then based on the discussions in [19], the measurement noise can usually be modeled as a finite sum of sinusoids, which can be described as:

$$\epsilon_j = \sum_{i=1}^{N_j} a_{ji} \sin(\omega_{ji} t + \varphi_{ji}), \quad j = 1, 2, \tag{23}$$

where $N_j > 0$ and ω_{ij} denotes the basic frequencies, $a_{ji} > 0$ and φ_{ij} denote the amplitude and the phase of each component, respectively. In this case, we have $\Xi_1 = \kappa^{-1}(\sum_{i=1}^{N_1} a_{1i}\omega_{1i} + \sum_{i=1}^{N_2} a_{2i})$. Hence, give some $\omega_i \geq \omega_\kappa = \kappa^{-1}$, it is found that the estimation error associated with P_2 will be significantly increased when a small κ is selected, in particular for high-frequency noise. This observation motivates the current study on further modification of USDE to enhance its robustness against high-requency noise.

IV. ENHANCED UNKNOWN SYSTEM DYNAMICS ESTIMATOR

In this section, we will develop an enhanced unknown system dynamics estimator (EUSDE) to suppress the effects of measurement noise encountered in the practice. For this purpose, Assumpiton 1 can be reformulated as:

Assumption 2: The unknown dynamics h satisfies r-th order local Lipschitz condition, thus there exists positive constant $\hbar_i > 0$ such that $\sup_{t\geq 0} |h^{(i)}| \leq \hbar_i$ is fulfilled.

The key idea is to introduce cascaded high-order filter operations in the design of USDE. By defining $z = [z_1, \cdots, z_r]^\top$ and $\psi = [\psi_1, \cdots, \psi_r]^\top$. Then the filter (14) can be repeated and reformulated as a higher-order form as:

$$\dot{z} = \frac{1}{\kappa} A z + \frac{1}{\kappa} B \bar{x}_2, \quad \dot{\psi} = \frac{1}{\kappa} A \psi + \frac{1}{\kappa} B \bar{\upsilon}, \tag{24}$$

with

$$A = \begin{bmatrix} -1 & 0 & 0 & \cdots & 0 & 0 \\ 1 & -1 & 0 & \cdots & 0 & 0 \\ 0 & 1 & -1 & \cdots & 0 & 0 \\ \vdots & \vdots & \vdots & \ddots & \vdots & \vdots \\ 0 & \cdots & \cdots & \cdots & 1 & -1 \end{bmatrix} \in \mathbb{R}^{r\times r},$$
$$B = \begin{bmatrix} 1 & 0 & \cdots & 0 \end{bmatrix}^\top \in \mathbb{R}^r, \tag{25}$$

where $r \geq 2$ is a manually set constant denoting the order of filters. Clearly, a cascaded high-order filter operation is applied on the measurements $\bar{x}_2, \bar{\upsilon}$ as defined in (24) to eliminate the influence of the perturbed measurement noise.

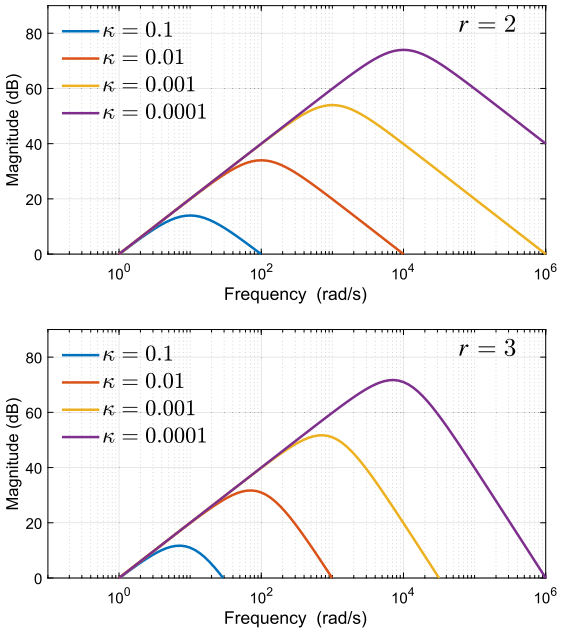

FIGURE 3. The frequency response of P_5 with EUSDE (26).

Then, the EUSDE can be designed as:

$$\hat{h} = \frac{z_{r-1} - z_r}{\kappa} - \psi_r. \tag{26}$$

Now, the performance of EUSDE (26) is first investigated via the frequency-domain analysis. Similar to those derivations given in (16), we can obtain the estimation error of EUSDE (26) in the frequency-domain as:

$$\tilde{H} = P_4 H - P_5 E_1 + P_6 E_2,$$
$$P_4 = 1 - \frac{1}{(\kappa s + 1)^r}, \; P_5 = \frac{s}{(\kappa s + 1)^r}, \; P_6 = \frac{1}{(\kappa s + 1)^r}. \tag{27}$$

As shown in (27), we know that the effects of E_1, E_2 on the estimation error $\tilde{H}$ can be suppressed by setting $r \geq 2$. To better show this fact, the frequency response of P_5 with $r = 2, 3$ is shown in Fig. 3. Compared with P_2 shown in Fig. 2, one can find that when $\omega_i \geq \omega_\kappa = \kappa^{-1}$, the magnitude of error transfer functions P_5 associated with the measurement noise E_1 could be eliminated with this configuration, since there is an asymptotic line with the slope of -20 dB/decade for $r = 2$ (or -40 dB/decade for $r = 3$). Similar observation can also be found for P_6 associated with the noise E_2.

On the other hand, the convergence of EUSDE (26) in the time-domain can be summarized as follows:

Theorem 3: Considering system (2) with measurement noise (12) and (13) with (23), then the estimation error $\tilde{h}$ of EUSDE (26) will ultimately converge to a compact set, whose size can be set small with proper r, κ.

Proof: Consider the change of coordinates:

$$e_r = \tilde{h}, \quad e_{r-1} = \dot{e}_r, \quad \ldots, \quad e_1 = \dot{e}_2, \tag{28}$$

with $e = [e_1, e_2, \ldots, e_r]$.

Based on (27), the estimation error $\tilde{h}$ can be represented in the time-domain as:

$$\dot{e} = \Lambda e + B\gamma, \quad \tilde{h} = Ce, \tag{29}$$

$$\gamma = \alpha_r^{-1}(\sum_{i=0}^{r-1} \alpha_{r-i} h^{(i+1)} - \dot{\epsilon}_1 + \epsilon_2), \tag{30}$$

where α_r is given by $(\kappa s + 1)^r = \alpha_r s^r + \ldots + \alpha_1 s + 1$ and

$$\Lambda = \begin{bmatrix} -\frac{\alpha_{r-1}}{\alpha_r} & -\frac{\alpha_{r-2}}{\alpha_r} & \cdots & -\frac{\alpha_1}{\alpha_r} & -\frac{1}{\alpha_r} \\ 1 & 0 & \cdots & 0 & 0 \\ 0 & 1 & \cdots & 0 & 0 \\ \vdots & \vdots & \ddots & \vdots & \vdots \\ 0 & 0 & \cdots & 1 & 0 \end{bmatrix},$$
$$C = \begin{bmatrix} 0 & 0 & \cdots & 1 \end{bmatrix}. \tag{31}$$

Given the fact that Λ is Hurwitz, there exist positive definite matrices $P > 0, Q > 0$, such that $Q = P\Lambda + \Lambda^\top P > 0$ is true.

Choosing a Lyapunov function as:

$$V_3 = \frac{1}{2}\tilde{h}^2 = e^\top C^\top P C e. \tag{32}$$

Then the time derivative of V_3 can be calculated along with (29) as:

$$\begin{aligned} \dot{V}_3 &= -\frac{1}{2} e^\top C^\top (P\Lambda + \Lambda^\top P) C e + e^\top C^\top P C B \gamma \\ &= -\frac{1}{2} e^\top C^\top Q C e + e^\top C^\top P C B \gamma, \end{aligned} \tag{33}$$

By using the Young's inequality, one can get:

$$e^\top C^\top P C B \gamma \le \frac{e^\top C^\top P^2 C e}{2\eta} + \frac{\eta C^\top B^\top B C \gamma^2}{2} \tag{34}$$

for a positive constant $\eta > 0$. Then, $\dot{V}_3$ can be derived as:

$$\dot{V}_3 \le -\sigma V_3 + \frac{\eta}{2} C^\top B^\top B C \Xi_2^2, \tag{35}$$

with

$$\sigma = \frac{\lambda_{\min}(Q)}{\lambda_{\max}(P)} - \frac{\lambda_{\max}(P)}{2\eta},$$
$$\Xi_2 = \alpha_r^{-1}(\sum_{i=0}^{r-1} \alpha_{r-i} \hbar_{i+1} + \sum_{i=1}^{N_1} a_{1i}\omega_{1i} + \sum_{i=1}^{N_2} a_{2i}). \tag{36}$$

Then we can claim that the estimation error $\tilde{h}$ converges to a compact set defined by:

$$\Omega_3 = \left\{ \tilde{h} \mid |\tilde{h}|^2 \le 2e^{-\sigma t}|\tilde{h}(0)|^2 + \sigma^{-1}\eta C^\top B^\top B C \Xi_2^2 \right\}. \tag{37}$$

Thus, for the proposed EUSDE (26), the estimation error $\tilde{h}$ is uniformly ultimately bounded, and the ultimate bound depends on the selection of κ and r. Compared with (20), as shown in (37), proper coefficient α_{r-i} depending on r, κ can be set, such that upper bound of Ω_3 can be tuned.

Remark 3: As shown in Theorem 3, the performance of the modified EUSDE can be improved by using a higher-order low-pass filter (24), where noise rejection is more apparent for higher order r. However, as the order of filter increases, the computational cost for implementing the EUSDE also increases. Moreover, the filter coefficient κ determining the bandwidth of filter should be taken as a tradeoff between the estimation accuracy and the robustness. As shown in [18], the bandwidth constraints become more strict as r increases. Nevertheless, the increase of r and κ may lead to a phase-lag in the estimator.

Remark 4: In our previous work [14], although a similar idea of using two-layer low-pass filters has been reported to address the problem of noise attenuation, the multiple filter coefficients may lead to a difficulty in implementation, which may also limit the application in SEAs. Besides, the introduced two-layer filter increases the complexity of convergence analysis. In this paper, a higher-order filter is applied where only two parameters κ and r are considered. Meanwhile, a comparative analysis from both the time-domain and frequency-domain perspectives is provided to illustrate the effectiveness of the proposed approach.

V. SIMULATIONS AND EXPERIMENTS

A. SIMULATIONS

In the simulations, the SEA model (2) is used with the following parameters and two different inputs:

$$\begin{aligned} \phi &= -0.1x_1 - 0.01x_2 + 100u, \\ h &= 0.01x_1 - 0.005x_2 + 0.005x_1^2, \\ u_1 &= -0.001x_1 - 0.001x_2 + 0.1\sin 2t, \\ u_2 &= -x_1 + 10\sin 2t. \end{aligned} \tag{38}$$

To exemplify the robustness against measurement noise, the measurement noise perturbing both x_1 and x_2 are produced by using "Uniform Random Number" block in the MATLAB with the power 10^{-6}. Following the above theoretical analysis, a fair $\kappa = 0.05$ is used for all case studies for the purpose of fair comparison.

Both the USDE (15) and the EUSDE (26) are all tested under u_1 and u_2. Fig. 4-7 provide the profiles of system states with/without measurement noise and the corresponding estimation performances of unknown system dynamics. Fig. 4 provides the system state under input u_1. Fig. 5 gives the estimation results of USDE and EUSDE, respectively. It is found that similar estimation performance are obtained for both the USDE and EUSDE in the absence of measurement noise. However, when there exists measurement noise, the modified EUSDE with the cascaded filter operation can suppress the effects of measurement noise effectively and thus achieve a better estimation performance than the original USDE. More specifically, the EUSDE with $r = 3$ can obtained even further improved response than the case with $r = 2$. Similar observations can also be found for the case with u_2 as shown in Fig.6-Fig.7. In conclusion, the proposed EUSDE has less fluctuations in the estimation, but superior capability of rejecting the measurement noise over the traditional USDE. Moreover, with the increase of the filter

order r, the rejection of measurement noise is enhanced to obtain a smoother $\hat{h}$.

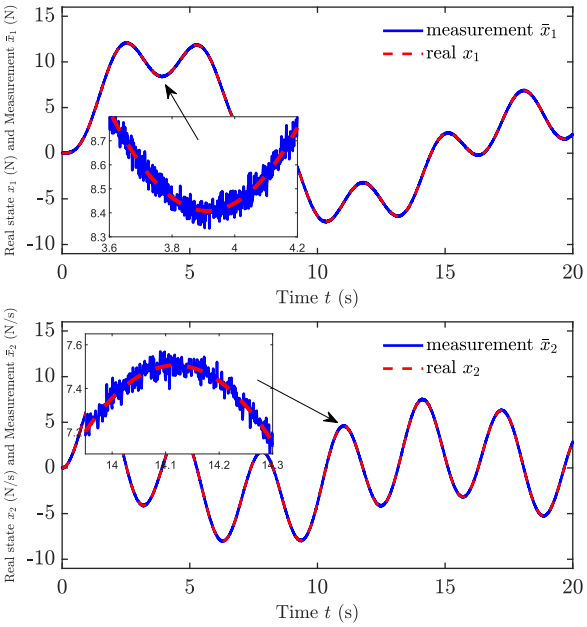

FIGURE 4. Profiles of state trajectories with u_1.

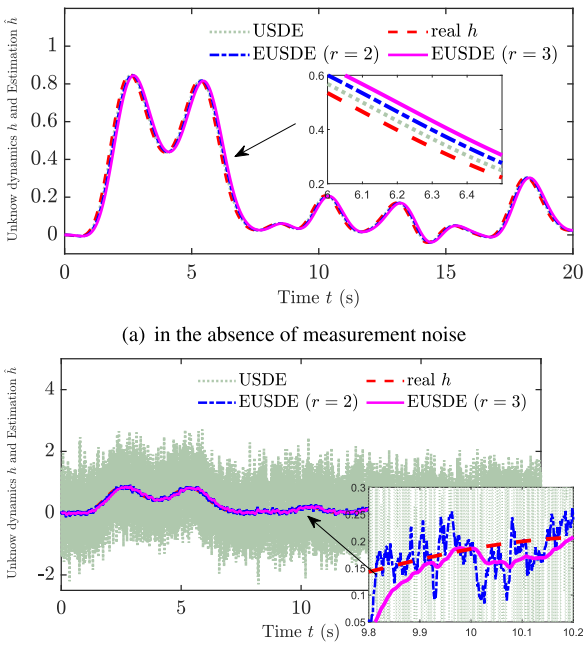

(a) in the absence of measurement noise

(b) in the presence of measurement noise

FIGURE 5. Estimation of unknown dynamics $h(t)$ with u_1.

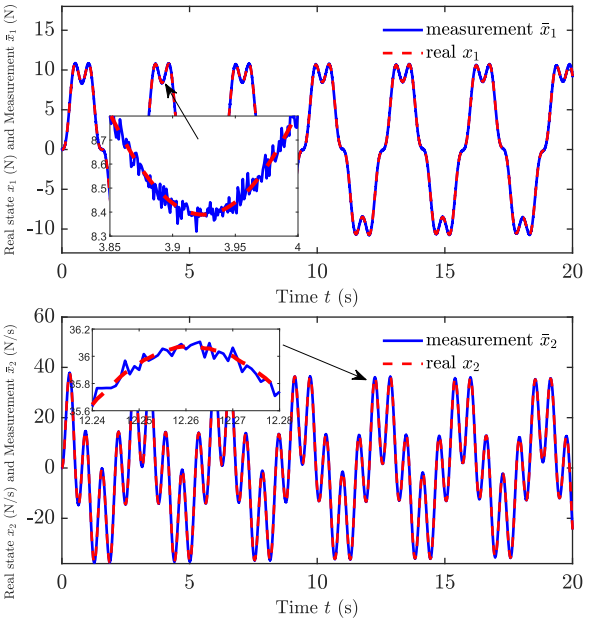

FIGURE 6. Profiles of state trajectories with u_2.

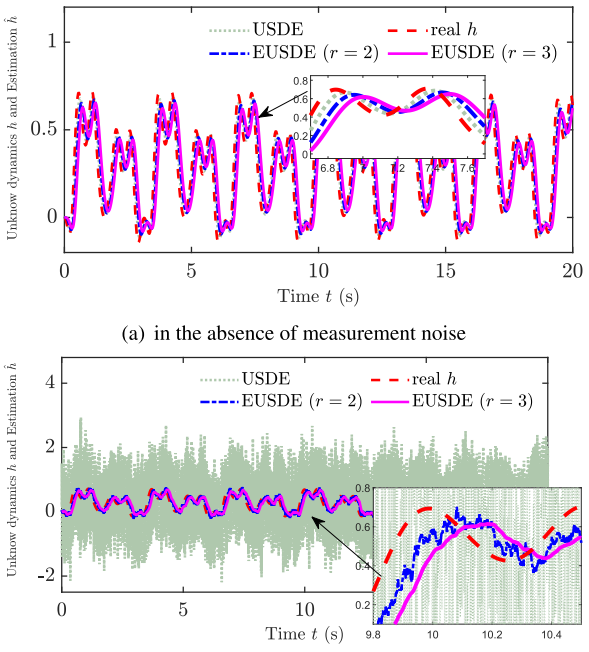

(a) in the absence of measurement noise

(b) in the presence of measurement noise

FIGURE 7. Estimation of unknown dynamics $h(t)$ with u_2.

B. EXPERIMENTS

In practical experiments, the prototype SEA manufactured in our lab is utilized as the test-rig, the diagram of which is given in Fig. 8. In this test-rig, a brushless DC motor (QDD Pro-NE30-50-70) embedded with a driver is applied as the actuator, which can provide 6600 mNm rated torque. The control algorithm is implemented in real-time based on an integrated controller with STM32F407ZGT6 and the sampling time is set as 50 ms. The output force of SEA is measured by an S-shaped force sensor with a sensor error of 0.2 N.

For the adopted SEA test-rig, a preliminary system identification phase has been carried out with input current

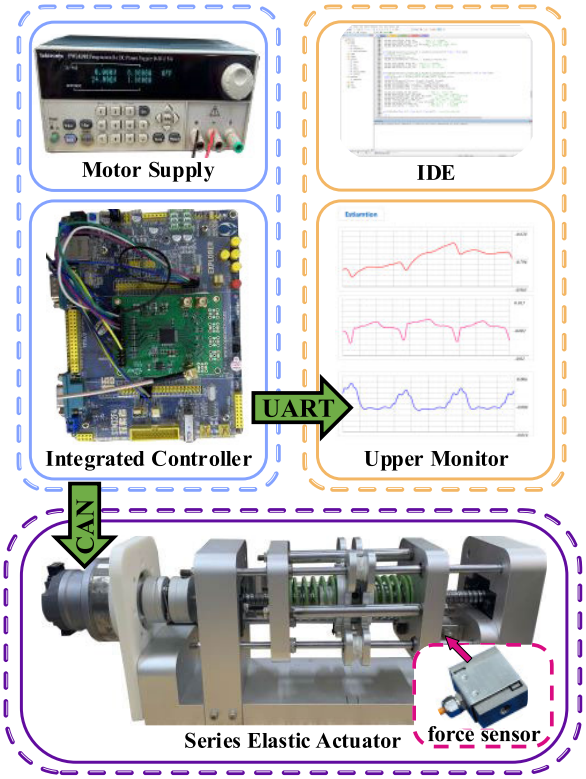

FIGURE 8. Experimental SEA Test-rig.

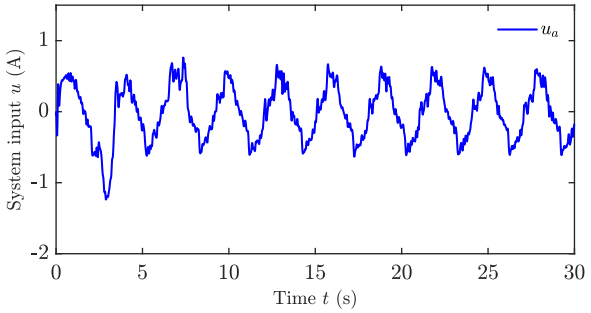

FIGURE 9. Input current u of SEA.

$u = 0.4 \sin \frac{2\pi}{3} t$ to obtain a baseline model described by:

$$\begin{cases} \dot{x}_1 = & x_2, \\ \dot{x}_2 = & -0.801x_1 - 0.415x_2 + 599.6u, \end{cases} \tag{39}$$

where the unknown system dynamics h is not considered. This model can be obtained by using the measured input u and output x_2 (gray solid line in Fig. 10), which can be reformulated as a linearized form given by:

$$\dot{x}_2 = \phi(x, u) = \theta\varphi, \tag{40}$$

where $\varphi = [-x_1, -x_2, u]^\top$ is the known regressor and $\theta = [0.801, 0.415, 599.6]$ is the parameter vector determined by the system identification via available input-output data.

The measured system output (gray solid line) and the output of baseline model (40) (blue dotted line) are depicted in Fig. 10, which indicates that there are clear difference between the ideal system output and the baseline model output, such that the baseline model (40) has significant modeling uncertainties, which should be further considered with the proposed estimators. Note that in this practice there is unavoidable measurement noise, and thus we test the performance of EUSDE (26). For this purpose, the EUSDE is implemented with parameters $\kappa = 0.02$ and $r = 6$ to reconstruct h, where the profile of estimated unknown dynamics is given in Fig. 11.

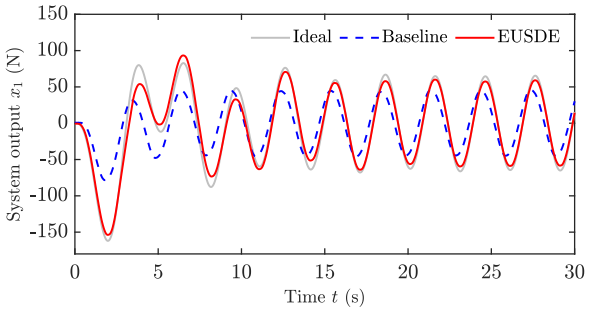

FIGURE 10. Responses of SEA (The gray solid line depicts the ideal measured system output; the blue dotted line depicts the system output derived from the baseline model; the red solid line depicts the system output with estimated unknown dynamics).

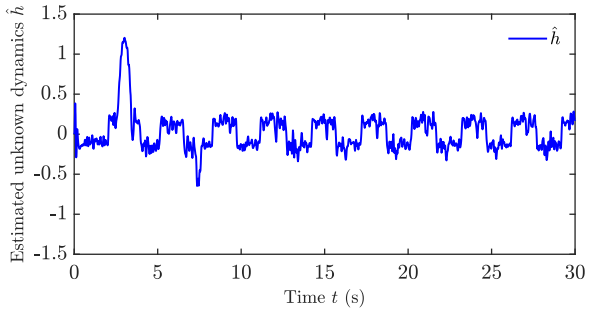

FIGURE 11. Estimated trajectory of unknown dynamics.

This estimated dynamics $\hat{h}$ is further incorporated to the baseline model to obtain a further improved model given by:

$$\dot{x}_2 = \phi(x, u) + \hat{h}, \tag{41}$$

where the output $\hat{h}$ of EUSDE is adopted as an extra compensation to the baseline model, i.e., $u = 0.4 \sin \frac{2\pi}{3} t + \frac{1}{\theta_3}\hat{h}$ as shown in Fig. 9, so as to exemplify the efficacy of the proposed UESDE by comparing the discrepancy between the measured system output, the output of baseline model (40) and modified model (41) (red solid line in Fig. 10).

From the experimental results given in Figs. 10-11, one can find that a reduced error is obtained between the measured SEA output and the modified model output (41) by incorporating the estimated dynamics $\hat{h}$ into the baseline model (40) in real-time. It should be noted that the peak

phenomenon occurring at $t = 3$s may be caused by the stiction friction and damping during the initiation operation phase. In this sense, it is found that the proposed EUSDE may also have the capability of achieving smooth and accurate estimations of piecewise continuous unknown dynamics, such as friction and damping.

VI. CONCLUSION

In this study, an EUSDE is designed by constructing a cascaded higher-order filter to online estimate the unknown system dynamics of the SEA systems. Different to our previous work on the design of USDE, the further modified EUSDE can suppress the sensitivity to measurement noise so as to achieve a better estimation performance. Comparative analysis concerning with the convergence performance and robustness to measurement noise of the USDE and EUSDE are rigorously studied in both the time-domain and frequency-domain. Comparative simulation results are given, which indicate that the developed EUSDE can maintain better estimation response than the USDE in the presence of measurement noise. Moreover, practical experiment results further reveal that the EUSDE can effectively compensate the unknown system dynamics involved in the adopted SEA test-rig and the discrepancy between the model output and the actual system output is further reduced by inserting the estimated dynamics into the baseline model. The proposed EUSDE can also enable the implementation of model-based controllers to achieve better control responses due to its simple structure and the estimation ability for unknown system dynamics.

REFERENCES

[1] G. Pratt and M. Williamson, "Series elastic actuators," in *Proc. IEEE/RSJ Int. Conf. Intell. Robots Syst. (IROS) Human Robot Interact. Cooperative Robots*, Aug. 1995, pp. 399–406.

[2] D. Ragonesi, S. Agrawal, W. Sample, and T. Rahman, "Series elastic actuator control of a powered exoskeleton," in *Proc. Annu. Int. Conf. IEEE Eng. Med. Biol. Soc.*, Boston, MA, USA, Aug. 2011, pp. 3515–3518.

[3] H. Yu, S. Huang, G. Chen, Y. Pan, and Z. Guo, "Human–robot interaction control of rehabilitation robots with series elastic actuators," *IEEE Trans. Robot.*, vol. 31, no. 5, pp. 1089–1100, Oct. 2015.

[4] S. Li, J. Li, G. Tian, and H. Shang, "Stiffness adjustment for a single-link robot arm driven by series elastic actuator in muscle training," *IEEE Access*, vol. 7, pp. 65029–65039, 2019.

[5] J. Vantilt, K. Tanghe, M. Afschrift, A. K. B. D. Bruijnes, K. Junius, J. Geeroms, E. Aertbeliën, F. De Groote, D. Lefeber, I. Jonkers, and J. De Schutter, "Model-based control for exoskeletons with series elastic actuators evaluated on sit-to-stand movements," *J. NeuroEng. Rehabil.*, vol. 16, no. 1, p. 65, Jun. 2019.

[6] W.-H. Chen, J. Yang, L. Guo, and S. Li, "Disturbance-observer-based control and related methods—An overview," *IEEE Trans. Ind. Electron.*, vol. 63, no. 2, pp. 1083–1095, Feb. 2016.

[7] K. Ohishi, "Torque-speed regulation of DC motor based on load torque estimation," in *Proc. IEEJ IPEC*, Tokyo, Japan, 1983, pp. 1209–1216.

[8] J. Han, "From PID to active disturbance rejection control," *IEEE Trans. Ind. Electron.*, vol. 56, no. 3, pp. 900–906, Mar. 2009.

[9] H. Chen, X. Shao, L. Xu, and R. Jia, "Finite-time attitude control with chattering suppression for quadrotors based on high-order extended state observer," *IEEE Access*, vol. 9, pp. 159724–159733, 2021.

[10] N. Paine, S. Oh, and L. Sentis, "Design and control considerations for high-performance series elastic actuators," *IEEE/ASME Trans. Mechatronics*, vol. 19, no. 3, pp. 1080–1091, Jun. 2014.

[11] H. Yu, S. Huang, G. Chen, and N. Thakor, "Control design of a novel compliant actuator for rehabilitation robots," *Mechatronics*, vol. 23, no. 8, pp. 1072–1083, Dec. 2013.

[12] S. Han, H. Wang, Y. Tian, and H. Yu, "Enhanced extended state observer-based model-free force control for a series elastic actuator," *Mech. Syst. Signal Process.*, vol. 183, Jan. 2023, Art. no. 109584.

[13] J. Na, A. S. Chen, Y. Huang, A. Agarwal, A. Lewis, G. Herrmann, R. Burke, and C. Brace, "Air-fuel ratio control of spark ignition engines with unknown system dynamics estimator: Theory and experiments," *IEEE Trans. Control Syst. Technol.*, vol. 29, no. 2, pp. 786–793, Mar. 2021.

[14] J. Yang, J. Na, H. Yu, G. Gao, and X. Wang, "Unknown system dynamics estimator for nonlinear uncertain systems," *IFAC-PapersOnLine*, vol. 53, no. 2, pp. 554–559, 2020.

[15] J. Na, J. Yang, S. Wang, G. Gao, and C. Yang, "Unknown dynamics estimator-based output-feedback control for nonlinear pure-feedback systems," *IEEE Trans. Syst., Man, Cybern., Syst.*, vol. 51, no. 6, pp. 3832–3843, Jun. 2021.

[16] J. Na, B. Jing, Y. Huang, G. Gao, and C. Zhang, "Unknown system dynamics estimator for motion control of nonlinear robotic systems," *IEEE Trans. Ind. Electron.*, vol. 67, no. 5, pp. 3850–3859, May 2020.

[17] X. Zhang, J. Mu, and C. Jing, "Adaptive control with unknown system dynamics estimator for quadrotor attitude tracking," *IEEE Access*, vol. 10, pp. 55102–55111, 2022.

[18] E. Sariyildiz and K. Ohnishi, "A guide to design disturbance observer," *J. Dyn. Syst., Meas., Control*, vol. 136, no. 2, Dec. 2013.

[19] D. Astolfi, L. Zaccarian, and M. Jungers, "On the use of low-pass filters in high-gain observers," *Syst. Control Lett.*, vol. 148, Feb. 2021, Art. no. 104856.

[20] J. Na, G. Herrmann, R. Burke, and C. Brace, "Adaptive input and parameter estimation with application to engine torque estimation," in *Proc. 54th IEEE Conf. Decis. Control (CDC)*, Japan, Dec. 2015, pp. 3687–3692.

[21] H. Khalil, *Nonlinear Systems*. Upper Saddle River, NJ, USA: Prentice-Hall, 2002.

CHENGHUAN LI received the B.S. degree in nanotechnology and materials from the Minzu University of China, Beijing, China, in 2019. He is currently pursuing the M.S. degree in system engineering with the Faculty of Information Engineering and Automation, Kunming University of Science and Technology, Kunming, China. His main research interest includes adaptive control and application.

SIYU CHEN received the B.S. degree in automation from Beijing University of Posts and Telecommunications, Beijing, in 2015. He is currently pursuing the Ph.D. degree in mechanical and electronic engineering with Kunming University of Science and Technology, Kunming, China. His current research interests include modeling, adaptive parameter estimation, and disturbance observer-based control.

JING NA (Member, IEEE) received the B.S. and Ph.D. degrees in automation and control from the School of Automation, Beijing Institute of Technology, Beijing, China, in 2004 and 2010, respectively. From 2011 to 2013, he was a Monaco/ITER Postdoctoral Fellow with ITER Organization, Saint-Paul-lez-Durance, France. From 2015 to 2017, he was a Marie Curie Fellow with the Department of Mechanical Engineering, University of Bristol, Bristol, U.K. Since 2010, he has been with the Faculty of Mechanical and Electrical Engineering, Kunming University of Science and Technology, Kunming, China, where he became a Professor, in 2013. He has coauthored one monograph and more than 100 international journal articles and conference papers. His current research interests include intelligent control, adaptive parameter estimation, nonlinear control, applications for robotics, vehicle systems, and wave energy converters.

He received several prestigious awards, including the Marie Curie Fellow, in 2015; the Hsue-Shen Tsien Paper Award, in 2017; and the Fok Ying Tung Award, in 2021. He has served as the Organization Committee Chair for the tenth Data Driven Control and Learning Systems Conference (DDCLS 2019) and the 33rd Chinese Control and Decision Conference (CCDC 2021). He is currently an Associate Editor of IEEE TRANSACTIONS ON INDUSTRIAL ELECTRONICS and the *Neurocomputing*.

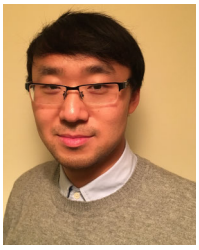

YINGBO HUANG received the B.S. degree from Lanzhou City University, China, in 2013, and the Ph.D. degree from the Faculty of Mechanical and Electrical Engineering, Kunming University of Science and Technology, Kunming, China, in 2019.

He is currently an Associate Professor of mechanical and electrical engineering with Kunming University of Science and Technology. His current research interest includes adaptive control and transient performance improvement of nonlinear control systems with application to vehicle suspension systems.

JUN MA received the Ph.D. degree from the Faculty of Information Engineering and Automation, Kunming University of Science and Technology, Kunming, China, in 2016. He was a Postdoctoral Researcher with the Faculty of Mechanical Engineering, Kunming University of Science and Technology, from 2016 to 2018, where he is currently an Associate Professor with the Faculty of Information Engineering and Automation. His research interests include fault diagnosis, prognostics, and health management.